

# High-frequency rectification in graphene lateral $p$ - $n$ junctions

Yu. B. Vasilyev,<sup>1</sup> G. Yu. Vasileva,<sup>1</sup> S. Novikov,<sup>2</sup> S. A. Tarasenko,<sup>1</sup> S. N. Danilov,<sup>3</sup> and S. D. Ganichev,<sup>3</sup>

<sup>1</sup>*Ioffe Institute, 194021 St. Petersburg, Russia*

<sup>2</sup>*Micro and Nanoscience Laboratory, Aalto University, Tietotie 3, FIN-02150, Espoo, Finland and*

<sup>3</sup>*Terahertz Center, University of Regensburg, 93040 Regensburg, Germany*

We observe a  $dc$  electric current in response to terahertz radiation in lateral inter-digitated double-comb graphene  $p$ - $n$  junctions. The junctions were fabricated by selective ultraviolet irradiation inducing  $p$ -type doping in intrinsic  $n$ -type epitaxial monolayer graphene. The photocurrent exhibits a strong polarization dependence and is explained by electric rectification in  $p$ - $n$  junctions.

The development of graphene electronic circuits is one of the important tasks of modern solid-state electronics. Doping or electrical gating of graphene enable the fabrication of  $p$ - $n$  junctions, which are the subject of intensive study, see e.g. [1–5]. It was found experimentally that graphene structures with lateral  $p$ - $n$  junctions demonstrate almost symmetric current-voltage ( $I$ - $V$ ) characteristics, which are very similar for the negative and positive polarities of the source-drain voltage [1–4]. The bi-directional charge transport is attributed to the Klein tunneling of Dirac fermions [6]. The symmetric character of the  $I$ - $V$  characteristic results in a lack of a pronounced rectification of electric signals in graphene  $p$ - $n$  devices being an obstacle for their application in electronics.

In optical measurements, however, it was observed that the illumination of graphene  $p$ - $n$  junctions leads to an electric response, which is a prerequisite for the fabrication of photodiodes [7, 8]. At high photon energy the photoresponse is caused by the creation of electron-hole pairs, which are separated by a built-in electric field of the  $p$ - $n$  junction [9]. This mechanism, however, fails for lower frequencies of terahertz (THz) range, for which the photon energy is typically much lower than the Fermi energy and the generation of electron-hole pairs is blocked. Nevertheless, irradiating sharp lateral graphene  $p$ - $n$  junctions by THz laser radiation we observe a  $dc$  current. The photocurrent is detected in epitaxial graphene on a SiC substrate with inter-digitated dual-comb  $p$ - $n$  junctions and is characterized by a strong dependence on the radiation polarization. The observations suggest the rectification of THz electric field in graphene  $p$ - $n$  junctions.

Epitaxial graphene samples for the subsequent  $p$ - $n$  junction fabrication were prepared by high-temperature Si sublimation of SiC [10]. In order to reduce the density of carriers we exposed the prepared samples in hot air [11]. This resulted in the initial  $n$ -type carrier density in the range  $(1.6 \div 3.1) \times 10^{11} \text{ cm}^{-2}$  and the mobility of about  $(1400 \div 2700) \text{ cm}^2/(\text{V s})$ . Then, the graphene was covered with polymers PMMA and ZEP500. This enable the adjusting of the carrier density by photochemical gating in which ZEP500 provide potent acceptors under deep ultraviolet (UV) light [12]. By irradiation with UV through the shadow mask graphene was patterned into  $p$ - $n$  structures consisting of inter-digitated finger stripes

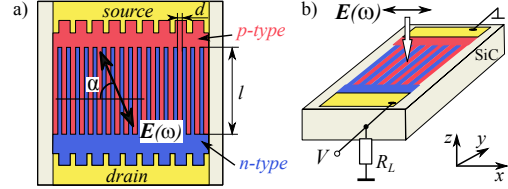


FIG. 1: (a) Top view of graphene photodiode, where the source and drain electrodes (yellow) are in contact with the  $p$ - (red) and  $n$ -type (blue) areas. (b) Experimental setup.

of  $p$ - and  $n$ -types, see Fig. 1. The irradiation dose was chosen high enough to inverse the carrier type from  $n$ - to  $p$ -type [13]. Consequently,  $p$ - $n$  junctions are formed along the boundary of the illuminated and not illuminated areas. Inter-digitated devices with finger length  $l = 1.8 \text{ mm}$  and width of  $d = 50$  and  $100 \mu\text{m}$  for samples #A (68 junctions), and #B (34 junctions), respectively, were fabricated to enlarge the area of the  $p$ - $n$  junctions. The type and degree of doping in the fingers were extracted from the Hall measurements. The obtained carrier densities are  $3 \times 10^{11} \text{ cm}^{-2}$  for the  $n$ -doped part and  $5 \times 10^{10} \text{ cm}^{-2}$  for the  $p$ -doped part. The corresponding Fermi energies  $E_F$  are 70 and 25 meV, respectively.

The experiments on photocurrents are performed applying radiation of  $\text{NH}_3$  laser [14, 15] operating at the frequencies  $f = 2$  and  $1.1 \text{ THz}$ . We use single pulses with a peak power of  $P \approx 10 \text{ kW}$ , a duration of about 100 ns and a repetition rate of 1 Hz. The beam had an almost Gaussian shape, as measured by a pyroelectric camera [16], and was focused at a spot with the diameter  $\approx 2 \text{ mm}$ . All experiments are performed at normal incidence of radiation, Fig. 1(b), and temperature  $T = 4.2 \text{ K}$ . We use linearly polarized radiation with the direction of the radiation electric field  $\mathbf{E}$  relative to the  $p$ - $n$  junction described by the angle  $\alpha$ , see Fig. 1(a). The latter was varied applying  $\lambda/2$ -plates [17].

First, we study  $I$ - $V$  characteristics applying  $dc$  voltage,  $V_{SD}$ , between the source and drain contacts, see Fig. 2. The data reveal that there is no asymmetry in the behavior of the current for the forward- and reverse-biased junctions. The symmetry indicates that our graphene structures as a whole do not exhibit rectifying properties, which is in contrast to conventional diodes based

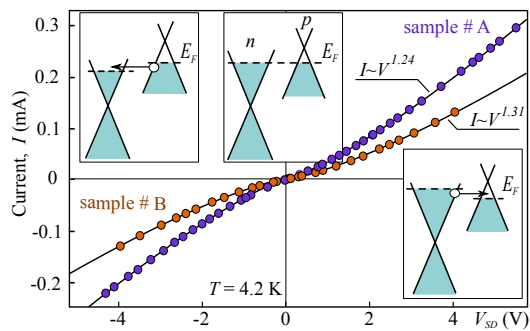


FIG. 2:  $I$ - $V$  characteristics. Insets illustrate the mechanism of the current flow in direct- and reverse-biased  $p$ - $n$  junctions.

on gaped semiconductors. A substantial current flow at the reverse-biased  $p$ - $n$  junction is attributed to the absence of a band gap in graphene and the related efficient Klein tunneling [6]. The corresponding band diagrams, sketched in Fig. 2, show that the electric current can flow for both polarities of the applied voltage.

The ability of a graphene  $p$ - $n$  junction to conduct electric current in both directions, however, implies neither that the  $I$ - $V$  characteristic itself is symmetric nor that the  $p$ - $n$  junction cannot rectify  $ac$  electric fields. In fact, the real  $I$ - $V$  characteristic of the  $p$ - $n$  junction and its possible asymmetry can be hidden in transport experiments and its measurement in the lateral graphene  $p$ - $n$  junction is a challenging task. This is because the current in such samples is determined by the large resistance of the  $p$ - and  $n$ -type areas rather than the small resistance of the thin  $p$ - $n$  junction. Note, in vertical graphene  $p$ - $n$  junctions, where the lateral resistance of the  $p$ -type and  $n$ -type areas does not play a role, an asymmetry of the  $I$ - $V$  characteristic was indeed observed [18, 19].

The conclusion that the  $I$ - $V$  characteristics in our lateral graphene samples are determined by the  $p$ - and  $n$ -type areas is supported by the fact that they are well described by the dependence  $I \propto V^\delta$  with  $1 < \delta < 1.5$ , see Fig. 2. Similar superlinear dependence was obtained earlier in experiments on homogeneous graphene samples and explained by the interplay of the intraband and interband contributions to the charge transport [20]. The dependence  $I \propto V^{1.5}$  also follows from theoretical calculations in the ballistic regime, see Refs. [21, 22].

To measure the response of the lateral  $p$ - $n$  junctions to a high-frequency electric field we excite the structure by THz radiation in the absence of an applied bias voltage (photovoltaic mode). Illuminating the structure at normal incidence we detect a  $dc$  photocurrent between the source and drain contacts which linearly scales with the radiation intensity and has a strong polarization dependence, see Fig. 3. The fact that the photoresponse emerges at normally incident radiation unambiguously indicates that it originates from the  $p$ - $n$  junction. Indeed, all known mechanisms of the photocurrent forma-

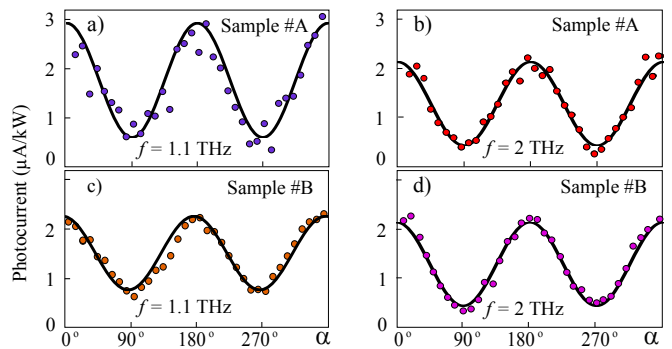


FIG. 3: Dependence of the photoresponse on the angle  $\alpha$  which determines the in-plane orientation of the THz electric field. The photoresponse is measured at the normal incidence of radiation in two samples for two different wavelengths.

tion in homogeneous graphene structures, such as photon drag or photogalvanic effect, require the oblique incidence of radiation or breaking the symmetry by a magnetic field [25, 26]. The photocurrent also cannot be caused by ratchet [27] or plasmonic [9] effects recently observed in graphene because they require metal gates superlattices.

The role of the  $p$ - $n$  junction also follows from the dependence of the photoresponse on the angle  $\alpha$  between the electric field of the radiation and the normal to the  $p$ - $n$  junctions, see 3. For both wavelengths studied the photocurrent reaches a maximum at  $\alpha = 0$  and  $180^\circ$ , when the  $ac$  electric field of the incident radiation is perpendicular to the  $p$ - $n$  junctions, and a minimum at  $\alpha = 90^\circ$ , when the radiation is polarized along the  $p$ - $n$  junctions. The overall polarization dependence is well fitted by

$$J(\alpha) = (a + b \cos^2 \alpha)P. \quad (1)$$

Note that the observed variation of the photoresponse is very large so that  $(J_{\max} - J_{\min})/(J_{\max} + J_{\min}) = 0.8 \div 0.9$  being close to unity. Furthermore, increasing the number of  $p$ - $n$  junctions by decreasing the width of the fingers in the combs (samples #A vs. #B) we observed an increase of the signal for low radiation frequencies. Comparing the photocurrent excited by  $f = 1.1$  and 2 THz radiation we see that in sample #A it decreases with raising frequency whereas in sample #B it remains unchanged.

Now we discuss the origin of the photoresponse. Since the energy of photons of THz radiation is much smaller than the Fermi energies of carriers in  $p$ -type and  $n$ -type areas, as well as in  $p$ - $n$  junction areas, the interband absorption of radiation with the creation of electron-hole pairs is blocked. In this case, the Drude absorption dominates and the quasi-classical approach to the description of electron transport through the  $p$ - $n$  junction becomes valid. The observed  $dc$  photocurrent can be interpreted as a result of the rectification: The  $ac$  electric field of the THz radiation incident upon the  $p$ - $n$  junction causes a high-frequency electric current, which is partially rectified due to the asymmetry of the  $I$ - $V$  characteristic of the

$p$ - $n$  junction. The rectification occurs in the area of the  $p$ - $n$  junction while, as discussed above, the homogenous  $p$ - and  $n$ -doped parts do not contribute to the formation of the  $dc$  signal. To the lowest order in the electric field amplitude, the  $dc$  current is described by the second order nonlinear term in the  $I$ - $V$  characteristic:

$$I_{dc} = \sigma_2 E_{\perp}^2, \quad (2)$$

where  $\sigma_2$  is the nonlinear conductance and  $E_{\perp}$  is the amplitude of the  $ac$  electric field across the  $p$ - $n$  junctions. The photocurrent scales quadratically with the electric field amplitudes as detected in experiment. The rectification mechanism also explains the observed polarization dependence. The  $dc$  electric current is generated by the component of the  $ac$  electric field normal to the  $p$ - $n$  junction varying as  $E_{\perp}^2 \propto \cos^2(\alpha)$  which is in agreement with the experimental data, Fig. 3. The presence of an additional small polarization-independent signal may be related to the photo-thermoelectric effect [28].

The observed weak frequency dependence of the photo-signal in sample #A and its absence in the sample #B are due to low mobility of carriers in our samples. Indeed, the frequency dependence is determined by the parameter  $\omega\tau$ , where  $\omega = 2\pi f$  and  $\tau$  is the momentum relaxation time. For the carrier density  $3 \times 10^{11} \text{ cm}^{-2}$ , mobility  $10^3 \text{ cm}^2/(\text{Vs})$ , and the radiation frequency  $f = 1 \text{ THz}$ , the estimation yields  $\omega\tau \approx 0.05$ . It shows that the  $ac$  transport of carries induced by THz radiation in the  $p$ - $n$  junctions is, in fact, quasi-stationary and depends on the  $ac$  electric field amplitude rather than on its frequency.

In conclusion, we have reported photocurrent measurements in graphene lateral  $p$ - $n$  junctions formed by selective deep UV illumination the graphene monolayer fabricated on a SiC substrate. We have observed a pronounced photoresponse in the THz range, which has a strong dependence on the radiation polarization. The observations are explained by the rectification mechanism of the photocurrent formation in graphene  $p$ - $n$  junctions.

We thank V. Belkov and V. Kachorovskii for fruitful discussions. The support from the RFBR (16-02-00326), and the DFG (SFB 1277-A04) is acknowledged. S.T. acknowledges the support from the RSF (14-12-01067).

---

[1] J. R. Williams, L. DiCarlo, and C. M. Marcus, *Science* **317**, 638 (2007).  
 [2] T. Lohmann, K. von Klitzing, and J. H. Smet, *Nano Lett.* **9**, 1973 (2009).  
 [3] E. C. Peters, E. J. H. Lee, M. Burghard, and K. Kern, *Appl. Phys. Lett.* **97**, 193102 (2010).  
 [4] M. Z. Iqbal, Salma Siddique, M. W. Iqbal, and J. Eom, *J. Mater. Chem. C* **1**, 3078 (2013).  
 [5] X. Yu, Y. Shen, T. Liu, T. Wu, and Q. J. Wang, *Sci. Rep.* **5**, 12014 (2015).  
 [6] M. I. Katsnelson, K. S. Novoselov and A. K. Geim, *Nat. Physics* **2**, 620 (2006).

[7] N. M. Gabor, J. C. W. Song, Q. Ma, N. L. Nair, T. Taychatanapat, K. Watanabe, T. Taniguchi, L. S. Levitov, and P. Jarillo-Herrero, *Science* **334**, 648 (2011).  
 [8] M. C. Lemme, F. H. L. Koppens, A. L. Falk, M. S. Rudner, H. Park, L. S. Levitov, and C. M. Marcus, *Nano Lett.* **11**, 4134 (2011).  
 [9] F. H. L. Koppens, T. Mueller, Ph. Avouris, A. C. Ferrari, M. S. Vitiello, M. Polini, *Nat. Nanotech.* **9**, 780 (2014).  
 [10] S. Novikov, N. Lebedeva, K. Pierz, and A. Satrapinski, *IEEE Trans. Instrum. Meas.* **64**, 1533 (2015).  
 [11] S. Ryu, L. Liu, S. Berciaud, Y.-J. Yu, H. Liu, P. Kim, G. W. Flynn, and L. E. Brus, *Nano Lett.* **10**, 4944 (2010).  
 [12] S. Lara-Avila, K. Moth-Poulsen, R. Yakimova, T. Bjornholm, V. Fal'ko, A. Tzalenchuk, and S. Kubatkin, *Adv. Mater.* **23**, 878 (2011).  
 [13] S. Lara-Avila, K. Moth-Poulsen, R. Yakimova, T. Bjornholm, V. Fal'ko, A. Tzalenchuk, and S. Kubatkin, *Advanced Materials* **23**, 878 (2011).  
 [14] S. D. Ganichev, W. Prettl, and P. G. Huggard, *Phys. Rev. Lett.* **71**, 3882 (1993).  
 [15] P. Schneider, J. Kainz, S. D. Ganichev, V. V. Bel'kov, S. N. Danilov, M. M. Glazov, L. E. Golub, U. Rössler, W. Wegscheider, D. Weiss, D. Schuh, and W. Prettl, *J. Appl. Phys.* **96**, 420 (2004).  
 [16] V. Lechner, L. E. Golub, P. Olbrich, S. Stachel, D. Schuh, W. Wegscheider, V. V. Bel'kov, and S. D. Ganichev, *Appl. Phys. Lett.* **94**, 242109 (2009).  
 [17] M. P. Walser, U. Siegenthaler, V. Lechner, D. Schuh, S. D. Ganichev, W. Wegscheider, and G. Salis, *Phys. Rev. B* **86**, 195309 (2012).  
 [18] S. Kim, D. H. Shin, C. O. Kim, S. S. Kang, J. M. Kim, C. W. Jang, S. S. Joo, J. S. Lee, J. H. Kim, S.-H. Choi, and E. Hwang, *ACS Nano* **7**, 5168 (2013).  
 [19] L. Britnell, R. V. Gorbachev, A. K. Geim, L. A. Ponomarenko, A. Mishchenko, M. T. Greenaway, T. M. Fromhold, K. S. Novoselov L. Eaves, *Nat. Commun.* **4**, 1794 (2013).  
 [20] N. Vandecasteele, A. Barreiro, M. Lazzeri, A. Bachtold, and F. Mauri, *Phys. Rev. B* **82**, 045416 (2010).  
 [21] M. Lasia, E. Prada, and L. Brey, *Phys. Rev. B* **85**, 245320 (2012).  
 [22] V. Ryzhii, I. Semenikhin, M. Ryzhii, D. Svintsov, V. Vyurkov, A. Satou, and T. Otsuji, *J. Appl. Phys.* **113**, 244505 (2013).  
 [23] J. Karch, P. Olbrich, M. Schmalzbauer, C. Zoth, C. Brinsteiner, M. Fehrenbacher, U. Wurstbauer, M. M. Glazov, S. A. Tarasenko, E. L. Ivchenko, D. Weiss, J. Eroms, R. Yakimova, S. Lara-Avila, S. Kubatkin, and S. D. Ganichev, *Phys. Rev. Lett.* **105**, 227402 (2010).  
 [24] S. A. Tarasenko, *Phys. Rev. B* **83**, 035313 (2011).  
 [25] C. Jiang, V. A. Shalygin, V. Y. Panevin, S. N. Danilov, M. M. Glazov, R. Yakimova, S. Lara-Avila, S. Kubatkin, and S. D. Ganichev, *Phys. Rev. B* **84**, 125429 (2011).  
 [26] C. Drexler, S. Tarasenko, P. Olbrich, J. Karch, M. Hirmer, F. Müller, M. Gmitra, J. Fabian, R. Yakimova, S. Lara-Avila, S. Kubatkin, M. Wang, R. Vajtai, P. Ajayan, J. Kono, S. D. Ganichev, *Nat. Nanotech.* **8**, 104 (2013).  
 [27] P. Olbrich, J. Kamann, M. König, J. Munzert, L. Tutsch, J. Eroms, D. Weiss, Ming-Hao Liu, L. E. Golub, E. L. Ivchenko, V. V. Popov, D. V. Fateev, K. V. Mashinsky, F. Fromm, Th. Seyller, and S. D. Ganichev, *Phys. Rev. B* **93**, 075422 (2016).  
 [28] M. Freitag, T. Low, and P. Avouris, *Nano Lett.* **13**, 1644 (2013).